**Ali TOFIGHI, Mohsen KALANTAR**

Iran University of Science and Technology

# Adaptive passivity-based control of PEM fuel cell/battery hybrid power source

***Abstract.*** *In this paper, a DC hybrid power source composed of PEM fuel cell as main source, Li-ion battery storage as transient power source and their power electronic interfacing is modelled based on Euler-Lagrange framework. Subsequently, Adaptive Passivity Based Controllers are synthesized using the energy shaping and damping injection techniques. In addition, the power management system is designed in order to manage power flow between components. The results show that the outputs of hybrid system have good tracking response, low overshoot, short settling time and zero steady-state error.*

*Streszczenie. Przedstawiono hybrydowy źródło DC składające się z ogniwa paliwowego typu PEM, baterii litowej i układu elektronicznego. Przeprowadzono syntezę adaptacyjnego pasywnego sterownika przy wykorzystaniu techniki kształtowania energii i tłumionego wtrysku. Dodatkowo kontroluje się przepływ mocy między komponentami. Otrzymano układ hybrydowy z dobrym śledzeniem obciążenia, małym przeregulowaniem i krótkim czasem ustalania. (**Adaptacyjny, bierny sterownik dla hybrydowego źródła mocy**)*

**Keywords:** Adaptive Passivity Based Control; DC hybrid power source; Fuel Cell; Li-Ion battery.
**Słowa kluczowe**: hybrydowe źródło mocy, bateria litowa

## I. Introduction

Distributed Generation (DG) has the advantages of low investment, low pollution, high efficiency, and high reliability. Fuel cells (FCs) are mostly being used due to some merits compared to the other types of DG sources [1]. However, one main disadvantage of fuel cell is its slow dynamics [2]. Hence, hybrid power sources are introduced to make the best use of its advantage and elimination of the aforementioned disadvantage [3-5]. Batteries are a secondary source which can supply power under transient conditions [6].

Fuel cells act as converters which convert the chemical energy into electrical energy [7]. Proton Exchange Membrance (PEM) fuel cell is a prime candidate for hybrid systems, because it has higher power density and lower operating temperature than the other types of FC systems [8].

Power electronic converters have a significant role in the hybrid systems [9]. These are interface between DG sources and other parts of hybrid system [7, 10]. Recently, some of researchers have concerned on control of hybrid power sources [11-13]. The methods of controller design classifies into two categories: linear and nonlinear. The linear methods performed relying on locally linearized models. Hence, their performance will not remain the same under any changes on equilibrium points. The PI controller is a main linear controller which is being used in DG applications [14-16]. The dynamic equations of the power electronic converters have a nonlinear nature due to the multiplications of the state variables by the control inputs [17,18]. Therefore, the nonlinear methods such as robust [19], feedback linearization [20], sliding mode [21], and passivity-based control [22,23] are used for control of converters. In particular, a passivity-based control method has taken into consideration in various industrial applications.

The Passivity-Based Control (PBC) was introduced, by Ortega et al., as a controller design methodology which achieves stabilization by passivation [24]. Two theories for PBC were developed which are: Euler-Lagrange (EL)-PBC [25] and Interconnection and Damping Assignment (IDA)-PBC [23]. These methods have been mostly used for control of induction motors [26], and switching power converters [27,28].

Lee has used EL-PBC for control of three phase AC/DC voltage source converter [29]. Also, a single phase PWM current source inverter control with applying IDA-PBC has been implemented by Komurcugil [30]. The control of fuel cell/ultracapacitor hybrid system has been achieved based on IDA-PBC by Ayad et al.[31].

In the most of hybrid systems, the value of the resistive load is constant but unknown. Therefore, adaptive type of controllers has been used to handle this type of uncertainty. Sira-Ramirez et al., has developed adaptive input-output linearization controller [32], and adaptive passivity based controller [33] for DC/DC converters.

The study in this paper is concentrated on the lagrangian modeling of fuel cell/battery DC hybrid power source, that the fuel cell is a main power source and battery storage is used as a transient power source. The control signals are achieved by adaptive passivity-based control. Power flow between hybrid system components is managed in the power management unit.

The paper is organized as follows. Section II introduces the hybrid DC power source and explains the suitable model of each component which is applied on hybrid system. Section III presents Euler-Lagrange model of DC hybrid power source. Adaptive passivity-based controllers design is achieved in section IV. Section V describes power management system. Section VI validates the proposed model by simulation results and section VII concludes the paper.

## II. Proposed System Description

The proposed hybrid power source is depicted in Fig. 1. This power source consists of a PEM fuel cell, Li-ion battery storage, DC/DC converters, adaptive passivity-based controllers, resistive load, and a power management center.

### A. PEM Fuel Cell Dynamic Model

A fuel cell is a static energy conversion device that converts chemical reaction of fuels directly into electrical energy. This energy conversion occurs whenever a fuel (hydrogen-rich gas) reacts chemically with the oxygen of air [3].

The suitable dynamic model of PEMFC is utilized in this study. Its equivalent circuit is depicted in Fig. 1 [1].

### B. Lithium-Ion Battery Model

Storage devices are used as energy storing in the hybrid power sources [34, 35]. The batteries store energy in the electrochemical form. Li-ion batteries are preferable to other types of batteries because they have high energy density, high operating voltage levels and long cycle life [36].

In this study, the dynamic model of Li-ion battery is utilized. That is a suitable model for Li-ion battery which predicts battery runtime and I-V performance accurately [37]. The aforementioned model of the Li-ion battery has been depicted in Fig. 1

**C. DC/DC converter**

The amplitude of DC output voltage of the fuel cell depends on both the internal electrochemical reaction and the external load impedance.

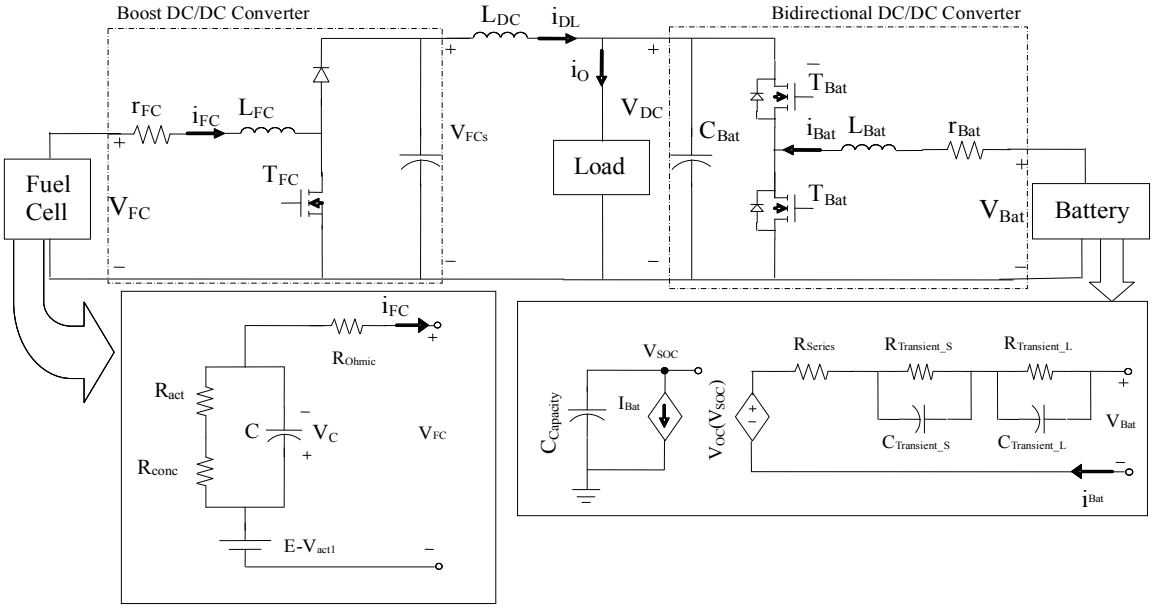


Fig. 1. Structure of proposed hybrid DC power source

Therefore, the boost DC/DC converter is used to regulate the output voltage of the fuel cell. Also, a bidirectional DC/DC converter is used to control the charging and discharging of the battery storage.

## III. Euler-Lagrange Model of Hybrid Power Source

In the previous sections, a suitable model for components of hybrid power source has been presented. In this section, the EL description of them is expressed.

The Lagrangian $\mathcal{L}(\dot{q},q)$ of the system is the difference of the magnetic co-energy of inductive elements, denoted by $\mathcal{T}(\dot{q},q)$, and the electric field energy of capacitive elements, denoted by $\mathcal{V}(q)$, i.e.

$$\mathcal{L}(\dot{q},q)=\mathcal{T}(\dot{q},q)-\mathcal{V}(q) \tag{1}$$

where $q$ is the vector of electric charges and $\dot{q}$ is the vector of flowing current. The EL modeling equations with consideration of circuit constraints is [25]:

$$\frac{d}{dt}\left(\frac{\partial \mathcal{L}}{\partial \dot{q}}(\dot{q},q)\right)-\frac{\partial \mathcal{L}}{\partial q}(\dot{q},q)=-\frac{\partial \mathcal{D}}{\partial \dot{q}}(\dot{q})+A(q)\lambda+\mathcal{F}_q \tag{2}$$

$$A(q)^T\dot{q}=0$$

where $\mathcal{D}(\dot{q})$ is the Rayleigh dissipation function, and $\mathcal{F}_q$ is the vector of generalized forcing functions.

In our case, the elements of the vector $q$, $\dot{q}$ consist electric charges $q_{C\_FC}$, $q_{C\_Bat}$, and $\dot{q}_{L\_FC}$, $\dot{q}_{L\_Bat}$, $\dot{q}_{L\_DC}$ corresponding to the fuel cell and battery DC/DC converter capacitors, and fuel cell, battery DC/DC converters and DC link inductors, respectively.

In the view of the hybrid system configuration represented in Fig. 1, the following EL equations:

$$\mathcal{T}=\frac{1}{2}\left(L_{FC}\dot{q}_{L\_FC}^2+L_{Bat}\dot{q}_{L\_Bat}^2+L_{DC}\dot{q}_{L\_DC}^2\right) \tag{3}$$

$$\mathcal{V}=\frac{1}{2}\left(\frac{1}{C_{FC}}q_{C\_FC}^2+\frac{1}{C_{Bat}}q_{C\_Bat}^2\right) \tag{4}$$

$$\mathcal{D}=\frac{1}{2}r_{FC}\dot{q}_{L\_FC}^2+\frac{1}{2}r_{Bat}\dot{q}_{L\_Bat}^2+\frac{1}{2}R_L\left[(1-u_{Bat})\dot{q}_{L\_Bat}+\dot{q}_{L\_DC}-\dot{q}_{C\_Bat}\right]^2 \tag{5}$$

$$\mathcal{F}_q=\begin{bmatrix}V_{FC} & V_{Bat} & 0 & 0 & 0\end{bmatrix}^T \tag{6}$$

where $r_i$ and $L_i$ is resistance and inductance of boosting inductor, respectively and $C_i$ is the capacity of the DC side filter capacitor, which $i=FC,Bat$ denote fuel cell and battery DC/DC converter, $R_L$ is load resistance.

The constraint equations are given by the Kirchhoff's current law, hence, the constraint matrix will be:

$$A=\begin{bmatrix}-(1-u_{FC}) & 0 & 1 & 1 & 0\end{bmatrix}^T \tag{7}$$

With definition $q=\begin{bmatrix}q_{L\_FC} & q_{L\_Bat} & q_{L\_DC} & q_{C\_FC} & q_{C\_Bat}\end{bmatrix}^T$ and considering (2) and (7), the EL equations are expanded as a set of scalar differential equations (8-12).

(8) $$\frac{d}{dt}(\frac{\partial \mathcal{L}}{\partial \dot{q}_{L\_FC}}(\dot{q}_{L\_FC}, q_{L\_FC})) - \frac{\partial \mathcal{L}}{\partial q_{L\_FC}}(\dot{q}_{L\_FC}, q_{L\_FC}) = -\frac{\partial \mathcal{D}}{\partial \dot{q}_{L\_FC}}(\dot{q}_{L\_FC}) - (1-u_{FC})\lambda + V_{FC}$$

(9) $$\frac{d}{dt}(\frac{\partial \mathcal{L}}{\partial \dot{q}_{L\_Bat}}(\dot{q}_{L\_Bat}, q_{L\_Bat})) - \frac{\partial \mathcal{L}}{\partial q_{L\_Bat}}(\dot{q}_{L\_Bat}, q_{L\_Bat}) = -\frac{\partial \mathcal{D}}{\partial \dot{q}_{L\_Bat}}(\dot{q}_{L\_Bat}) + V_{Bat}$$

(10) $$\frac{d}{dt}(\frac{\partial \mathcal{L}}{\partial \dot{q}_{L\_DC}}(\dot{q}_{L\_DC}, q_{L\_DC})) - \frac{\partial \mathcal{L}}{\partial q_{L\_DC}}(\dot{q}_{L\_DC}, q_{L\_DC}) = -\frac{\partial \mathcal{D}}{\partial \dot{q}_{L\_DC}}(\dot{q}_{L\_DC}) + \lambda$$

(11) $$\frac{d}{dt}(\frac{\partial \mathcal{L}}{\partial \dot{q}_{C\_FC}}(\dot{q}_{C\_FC}, q_{C\_FC})) - \frac{\partial \mathcal{L}}{\partial q_{C\_FC}}(\dot{q}_{C\_FC}, q_{C\_FC}) = -\frac{\partial \mathcal{D}}{\partial \dot{q}_{C\_FC}}(\dot{q}_{C\_FC}) + \lambda$$

(12) $$\frac{d}{dt}(\frac{\partial \mathcal{L}}{\partial \dot{q}_{C\_Bat}}(\dot{q}_{C\_Bat}, q_{C\_Bat})) - \frac{\partial \mathcal{L}}{\partial q_{C\_Bat}}(\dot{q}_{C\_Bat}, q_{C\_Bat}) = -\frac{\partial \mathcal{D}}{\partial \dot{q}_{C\_Bat}}(\dot{q}_{C\_Bat})$$

After a straightforward calculation of (8-12) with the EL parameters (13-17), the EL model equations are yielded in the following form:

(13) $$L_{FC}\ddot{q}_{L\_FC} + r_{FC}\dot{q}_{L\_FC} + (1-u_{FC})\frac{1}{C_{FC}}q_{C\_FC} = V_{FC}$$

(14) $$L_{Bat}\ddot{q}_{L\_Bat} + r_{Bat}\dot{q}_{L\_Bat} + (1-u_{Bat})\frac{1}{C_{Bat}}q_{C\_Bat} = V_{Bat}$$

(15) $$L_{DC}\ddot{q}_{L\_DC} - \frac{1}{C_{FC}}q_{C\_FC} + \frac{1}{C_{Bat}}q_{C\_Bat} = 0$$

(16) $$-(1-u_{FC})\ddot{q}_{L\_FC} + \dot{q}_{L\_DC} + \dot{q}_{C\_FC} = 0$$

(17) $$(1-u_{Bat})\ddot{q}_{L\_Bat} + \dot{q}_{L\_DC} - \dot{q}_{C\_Bat} - \frac{1}{R_L C_{Bat}}q_{C\_Bat} = 0$$

Which results with

$$z = \begin{bmatrix} i_{FC} & i_{Bat} & i_{DC} & V_{FCs} & V_{DC} \end{bmatrix}^T$$

$$= \begin{bmatrix} \dot{q}_{L\_FC} & \dot{q}_{L\_Bat} & \dot{q}_{L\_DC} & \frac{1}{C_{FC}}q_{C\_FC} & \frac{1}{C_{Bat}}q_{C\_Bat} \end{bmatrix}^T$$

in the state equation:

(18) $$L_{FC}\dot{z}_1 + r_{FC}z_1 + (1-u_{FC})z_4 = V_{FC}$$

(19) $$L_{Bat}\dot{z}_2 + r_{Bat}z_2 + (1-u_{Bat})z_5 = V_{Bat}$$

(20) $$L_{DC}\dot{z}_3 - z_4 + z_5 = 0$$

(21) $$C_{FC}\dot{z}_4 - (1-u_{FC})z_1 + z_3 = 0$$

(22) $$C_{Bat}\dot{z}_5 - (1-u_{Bat})z_2 - z_3 + \frac{z_5}{R_L} = 0$$

The aforementioned equations represent in the matrix form as:

(23) $$\mathcal{M}\dot{z} + \mathcal{T}(u)z + Rz = \mathcal{E}$$

$$\mathcal{M} = diag\{L_{FC};\ L_{Bat};\ L_{DC};\ C_{FC};\ C_{Bat}\}$$

$$\mathcal{R} = diag\left\{r_{FC};\ r_{Bat};\ 0;\ 0;\ \frac{1}{R_L}\right\}$$

(24) $$\mathcal{T} = \begin{bmatrix} 0 & 0 & 0 & 1-u_{FC} & 0 \\ 0 & 0 & 0 & 0 & 1-u_{Bat} \\ 0 & 0 & 0 & -1 & 1 \\ -(1-u_{FC}) & 0 & 1 & 0 & 0 \\ 0 & -(1-u_{Bat}) & -1 & 0 & 0 \end{bmatrix}$$

where $\mathcal{M}$ is a positive-definite diagonal matrix, $\mathcal{T}$ is the interconnection matrix, $\mathcal{R}$ is the dissipation matrix, and $\mathcal{E}$ is the vector consisting of voltage sources. The total energy function is:

(25) $$\mathcal{H}(t) = \mathcal{T} + \mathcal{V} = \frac{1}{2}z^T\mathcal{M}z$$

where satisfies the energy balance equation:

(26) $$\mathcal{H}(T) - \mathcal{H}(0) + \int_0^T z^T\mathcal{R}z dt = \int_0^T z^T\mathcal{E}dt$$

Which describes that the sum of the stored energy and dissipated energy equals the supplied energy.

The control objective for this hybrid system is a DC value of the output voltage of both DC/DC converters equal to a DC bus constant voltage.

Substitute $z_{4d} = z_{5d} = V_d$ in the dynamical equations (18-22) after some calculations the equilibrium vector is expressed as:

(27) $$z_d = \begin{bmatrix} z_{1d} & z_{2d} & z_{3d} & z_{4d} & z_{5d} \end{bmatrix}^T$$

In which $z_{id}, i = 1,2,...,5$, denote the desired constant equilibrium states of the closed loop system. Where

(28) $$z_{1d} = \frac{1}{2r_{FC}}\left[V_{FC} - \sqrt{V_{FC}^2 - 4r_{FC}V_d z_{3d}}\right]$$

$$z_{2d} = \frac{1}{2r_{Bat}}\left[V_{Bat} - \sqrt{V_{Bat}^2 - 4r_{Bat}V_d(\frac{V_d}{R_L} - z_{3d})}\right],\ z_{4d} = \frac{V_d}{R_L}$$

**IV. Adaptive Passivity-Based Controller design**

It is assumed that the resistive loads of hybrid system are constant, but are unknown. Therefore, to handle this type of uncertainty, adaptive passivity-based control is developed, on the other hands, the main objective is the load supplying only by the DC source. Therefore, the DC/DC converter of fuel cell is controlled to maintain the DC bus voltage to a constant value. The battery storage has been considered for instantaneous loads and whenever the load power exceeds the fuel cell rated power. Hence, in this condition, the DC bus voltage will be constant with controlling of DC/DC converter of battery storage.

The resistance load can be estimate by adaptation approach. Let

(29) $$\tilde{\theta} = \hat{\theta} - \theta\ ,\quad \frac{1}{R_L} = \theta$$

where $\hat{\theta}$ is the estimation value of $\theta$, $\tilde{\theta}$ is the estimation error.

Also, consider the error state vector:

$\tilde{z} = [\tilde{z}_1 \quad \tilde{z}_2 \quad \tilde{z}_3 \quad \tilde{z}_4 \quad \tilde{z}_5]^T$ ,The
$= [z_1 - z_{1d} \quad z_2 - z_{2d} \quad z_3 - z_{3d} \quad z_4 - z_{4d} \quad z_5 - z_{5d}]^T$
error dynamic equation is expressed as:

(30) $\mathcal{M}\dot{\tilde{z}} + \mathcal{J}(u)\tilde{z} + \mathcal{R}\tilde{z} = \mathcal{E} - (\mathcal{M}\dot{z}_d + \mathcal{J}(u)z_d + \mathcal{R}z_d)$

Adding $\mathcal{R}_a\tilde{z}$ to both sides of equations (30), the error dynamics with desired damping is:

(31) $\mathcal{M}\dot{\tilde{z}} + \mathcal{J}(u)\tilde{z} + \mathcal{R}_d\tilde{z} = \mathcal{E} - (\mathcal{M}\dot{z}_d + \mathcal{J}(u)z_d + \mathcal{R}z_d - \mathcal{R}_a\tilde{z})$

By considering the following desired error dissipation matrix:

(32) $\mathcal{R}_d = \mathcal{R} + \mathcal{R}_a$

where $\mathcal{R}$ from (24) rewritten as:

(33) $\mathcal{R} = diag\{r_{FC};\ r_{Bat};\ 0;\ 0;\ \hat{\theta}\}$

where the injected damping

(34) $\mathcal{R}_a = diag\{r_{a1};\ r_{a2};\ 0;\ 0;\ 0\}$

Supposing that the right-hand side of the equation (31) is:

(35) $\mathcal{M}\dot{\tilde{z}} + \mathcal{J}(u)\tilde{z} + \mathcal{R}_d\tilde{z} = \psi$

where

(36) $\psi = \mathcal{E} - (\mathcal{M}\dot{z}_d + \mathcal{J}(u)z_d + \mathcal{R}z_d - \mathcal{R}_a\tilde{z})$

Consider the total energy, (37), where $\gamma$ is the strictly positive constant, as a Lyapunov function:

(37) $\mathcal{H}_d(t) = \frac{1}{2}\tilde{z}^T\mathcal{M}\tilde{z} + \frac{1}{2\gamma}\tilde{\theta}^2$

For (37) the asymptotic stability of the error dynamic is achieved due to the positive definiteness of the matrix $\mathcal{M}$ and satisfying its derivative:

(38) $$\dot{\mathcal{H}}_d(t) = \tilde{z}^T\mathcal{M}\dot{\tilde{z}} + \frac{1}{\gamma}\tilde{\theta}\dot{\tilde{\theta}} = -\tilde{z}^T\mathcal{R}_d\tilde{z} + \left[(z_5 - z_{5d})z_{5d} + \frac{1}{\gamma}\dot{\tilde{\theta}}\right]\tilde{\theta}$$

Hence, the adaptive law:

(39) $(z_5 - z_{5d})z_{5d} + \frac{1}{\gamma}\dot{\tilde{\theta}} = 0$

Using the above equation and the fact that $\dot{\tilde{\theta}} = \dot{\hat{\theta}}$, the adaptive law will be:

(40) $\hat{\theta} = -\int[(z_5 - z_{5d})z_{5d}]dt$

Under this condition

(41) $\dot{\mathcal{H}}_d(t) = -\tilde{z}^T\mathcal{R}_d\tilde{z} \le -\alpha\mathcal{H}_d(t)$

where $\alpha$ is the strictly positive constant.
It is concluded that the error dynamics (35) are asymptotically stable towards the equilibrium point located at $z_{4d} = z_{5d} = V_d$.
Thus, in order to obtain desired error dynamics, and comparing (31), (35):

(42) $\psi = \mathcal{E} - \mathcal{M}\dot{z}_d - \mathcal{J}(u)z_d - \mathcal{R}z_d + \mathcal{R}_a\tilde{z}$

Using (28), (39) supposed:

(43) $\psi = [0 \quad 0 \quad 0 \quad 0 \quad \tilde{\theta}z_{5d}]^T$

Equation (42) is extended to the following scalar differential equations:

(44) $V_{FC} - L_{FC}\dot{z}_{1d} - r_{FC}z_{1d} - (1-u_{FC})z_{4d} + r_{a1}(z_1 - z_{1d}) = 0$

(45) $V_{Bat} - L_{Bat}\dot{z}_{2d} - r_{Bat}z_{2d} - (1-u_{Bat})z_{5d} + r_{a2}(z_2 - z_{2d}) = 0$

(46) $-L_{DC}\dot{z}_{3d} + z_{4d} - z_{5d} = 0$

(47) $-C_{FC}\dot{z}_{4d} + (1-u_{FC})z_{1d} - z_{3d} = 0$

(48) $-C_{Bat}\dot{z}_{5d} + (1-u_{Bat})z_{2d} + z_{3d} - \frac{z_{5d}}{R_L} = (\hat{\theta} - \frac{1}{R_L})z_{5d}$

The control objective of this study is the adaptive passivity-based control of DC output voltage, but the direct control is not feasible due to its lack of stability, see [38], hence, the indirect control is used for the regulation of output DC voltage to a constant equilibrium value.

Consider the equations of the boost DC/DC converter of fuel cell (44) and (47), the desired constant value for the fuel cell current (converter input current) is $z_{1d}$, from the first equation (44), the control variable $u_{FC}$ can be solved as:

(49) $u_{FC} = 1 - \frac{1}{z_{4d}}[V_{FC} - r_{FC}z_{1d} + r_{a1}(z_1 - z_{1d})]$

Substituting (49) into the Eq. (47), after a straightforward calculation, the controller state, $z_{4d}(t)$, can be achieved as:

(50) $\dot{z}_{4d} = \frac{1}{C_{FC}}\left[-z_{3d} + \frac{z_{1d}}{z_{4d}}(V_{FC} - r_{FC}z_{1d} + r_{a1}(z_1 - z_{1d}))\right]$

Also, consider the equations of DC/DC converter of battery storage (45) and (48), the desired constant value for the battery current is $z_{2d}$, the control variable $u_{Bat}$ can be solved from the second equation as:

(51) $u_{Bat} = 1 - \frac{1}{z_{5d}}[V_{Bat} - r_{Bat}z_{2d} + r_{a2}(z_2 - z_{2d})]$

Then substituting the control variable $u_{Bat}$ into the Eq. (48), yields the controller state, $z_{5d}(t)$,

(52) $$\dot{z}_{5d} = \frac{1}{C_{Bat}}\left[z_{3d} - \hat{\theta}z_{5d} + \frac{z_{2d}}{z_{5d}}(V_{Bat} - r_{Bat}z_{2d} + r_{a2}(z_2 - z_{2d}))\right]$$
$$\dot{\hat{\theta}} = -\gamma(z_5 - z_{5d})z_{5d}$$

Calculation of controller states, $z_{4d}(t)$ and $z_{5d}(t)$, depends on $z_{3d}$, which can be achieved as:

(53) $\dot{z}_{3d} = \frac{1}{L_{DC}}[z_{4d} - z_{5d}]$

**V. Power Management System**

In the proposed hybrid DC power source, the fuel cell and the battery storage have cooperation to supply the load. Hence, the Power Management System (PMS) needs to control the power flow between the fuel cell, battery storage and the load.
The power management system acts based on certain strategies; subsequently all of PMS strategies are explained:
(In this study, operation of battery storage has been considered based on SOC% situation between 40% and 80%)

1. Compute $P_e$ $(P_e = P_{FC\_rated} - P_{Load})$

2. If $P_e$ is positive and SOC %≤ 80%, then the fuel cell rated power is more than the load power. Also, the battery storage is in charge mode $(P_{FC\_gen} = P_{Load}, P_{Bat} = P_{FC\_rated} - P_{Load})$.
3. If $P_e$ is positive and SOC %> 80%, then the fuel cell rated power is more than load power. Also, the battery storage is not in safe charge mode $(P_{FC\_gen} = P_{Load}, \ P_{Bat} = 0)$.
4. If $P_e$ is negative and SOC %≥ 40%, then the fuel cell rated power is less than load power. Also, the battery storage is in discharge mode $(P_{FC\_gen} = P_{FC\_rated}, P_{Bat} = P_{Load} - P_{FC\_rated})$.
5. If $P_e$ is negative and SOC %< 40%, then the fuel cell rated power is less than load power. Also, the battery storage is not in safe discharge mode. Therefore, PMS apply load shading, and only supply load power based on rated power of fuel cell $(P_{Load} = P_{FC\_rated}, P_{Bat} = 0)$.

## VI. Simulation results and discussion

The propose of this paper is to address the Euler-Lagrange framework modeling and adaptive passivity-based control of FC/Battery hybrid power source. MATLAB/Simulink environment is used to investigate the performance of the adaptive passivity-based control on FC/Battery hybrid power source. The mathematical model of each component in the DC hybrid power source has been presented in the previous sections. It consists of dynamic model of fuel cell Stack, dynamic model of Li-ion battery, nonlinear models of DC/DC boost converter and bidirectional DC/DC converter, adaptive passivity-based Controllers and power management system. The specifications of SR-12 fuel cell Stack is shown in Table 1. The specifications of Li-ion battery storage are given in table 2. The DC/DC converters specifications are given in Table 3.

Table 1. Specifications of PEM Fuel Cell (SR-12) [1]

| Parameter | Value | Parameter | Value |
|---|---|---|---|
| A ($cm^2$) | 62.5 | $\eta_0(V)$ | 20.145 |
| $P_{O2}$ (atm) | 1.0 | $P_{H2}$ (atm) | 1.5 |
| a ($VK^{-1}$) | -0.1373 | b ($VK^{-1}$) | $7.48.10^{-5}$ |
| B (V) | 0.15 | $l$ (m) | $25.10^{-6}$ |
| $n_s$ | 48 | $R_C$ (ohm) | 0.0003 |
| $J_{max}$ ($mAcm^{-2}$) | 672 | C (F) | 4.8 |
| R ($Jmol^{-1}K^{-1}$) | 8.3143 | F ($Coulom^{-1}$) | 96487 |

Table 2. Specifications of Li-Ion Battery [39]

| Parameter | Value |
|---|---|
| Capacity (mAh) | 850 |
| Nominal Voltage (V) | 3.7 |
| Max. Charge Voltage (V) | 4.23 |
| Number of series Cell | 6 |
| Number of parallel strings | 4 |

Table 3. Specifications of DC/DC Converters

| Parameter | Value | Parameter | Value |
|---|---|---|---|
| $L_{FC}$(mH) | 23.2 | $L_{Bat}$ (mH) | 16 |
| $C_{FC}$ (μF) | 330 | $C_{Bat}$ (μF) | 87 |
| $r_{FC}$ (Ω) | 0.03 | $r_{Bat}$ (Ω) | 0.07 |

These simulations are achieved in the two cases:

I. The DC bus voltage reference is constant; moreover the initial SOC% of the battery storage is 70 (first case).
II. The DC bus voltage reference changes; the initial SOC% of the battery storage is 85 (second case).

The rated power of PEM fuel cell is 500 watt.

### A. First Case

The step change in resistance load is given in Fig. 2-a. The DC bus voltage reference is 100 Volt. The system response to change in resistance load is presented in the following Figs. The DC bus voltage $(V_{FCs})$, load voltage $(V_{DC})$ and voltage reference are shown in Fig. 2-b. Fig. 2-c presents load current $(I_o)$. The response of the DC voltage and load current exhibits a smooth and fast transient to a step change in the resistance load.

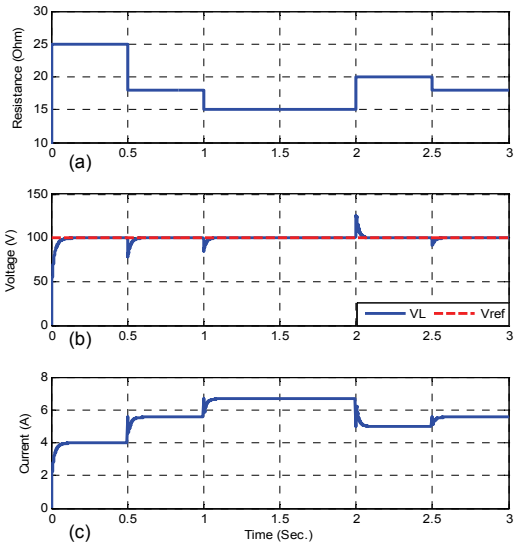


Fig. 2. (a). Load resistance, (b). DC bus, load voltage and DC bus voltage reference, (c). Load current

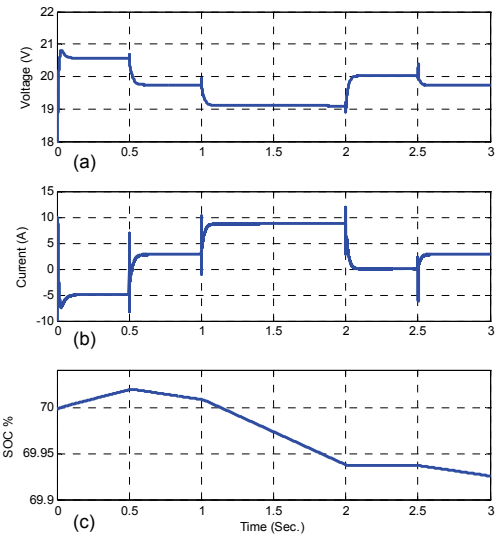


Fig. 3. (a). Battery voltage, (b). Battery current, (c). SOC of battery

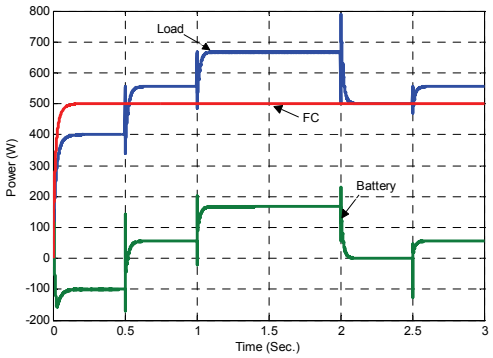


Fig. 4. Load, fuel cell and battery power

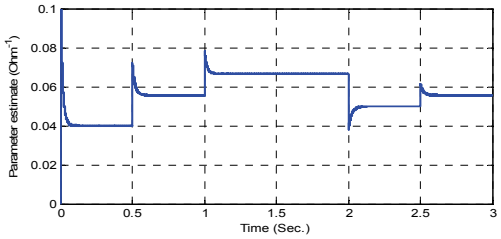


Fig. 5. Estimated value of $1/R_l$

This means that the hybrid system has a very good dynamic response to resistance load disturbance.

In this case, the fuel cell has a rated output. Therefore, voltage and current of the fuel cell is constant.

The battery storage voltage $(V_{Bat})$ and current $(I_{Bat})$ are shown in Figs 3-a and 3-b. According to PMS algorithm, the battery storage supply load in the transient conditions. Also, it supplies the remained load power when the load power is greater than fuel cell power rating.

Fig. 3-c presents the SOC of battery storage that the charging and discharging modes are demonstrated. In this case, the initial SOC% of battery storage is 70. Therefore, battery storage is in the discharging mode between (t=0.5 and t=2 sec, t=2.5 and t=3sec.). Because the load power exceeds from the fuel cell power rating. Therefore, the generated power of fuel cell is maximum. That is evident in Fig. 4.

The estimated value of resistance load is shown in Fig. 5.

**B. Second Case**

In the second case, the DC bus reference is not constant. Also, the initial SOC% of battery is 85. The step change in the resistance load is given in Fig. 6-a.

Fig. 6-b presents the system response to change in the DC bus voltage reference and load resistance. The DC bus voltage $(V_{FCs})$ and load voltage $(V_{DC})$ track well the voltage reference. It has zero steady state error. The load current $(I_o)$ is shown in Fig 6-c.

The fuel cell voltage $(V_{FC})$ and current $(I_{FC})$ are shown in Figs. 7-a and 7-b. Fuel cell have a rated power generation (between t=1.5 and t=3 sec.).

SOC% of the battery storage has been limited between 40 and 80. Therefore, based on PMS algorithm, it has no charging mode in this case. Figs. 8-a and 8-b present the battery storage voltage $(V_{Bat})$ and current $(I_{Bat})$. The SOC% of battery storage is presented in Fig. 8-c.

The power flow between components is shown in Fig. 9. Based on, it is evident that the transient power and the exceeded power from the fuel cell rated power are supplied by the battery storage. Moreover, it has no charging mode.

The estimated value of resistance load is shown in Fig. 10 which demonstrates that the estimated value converges very close to the true values.

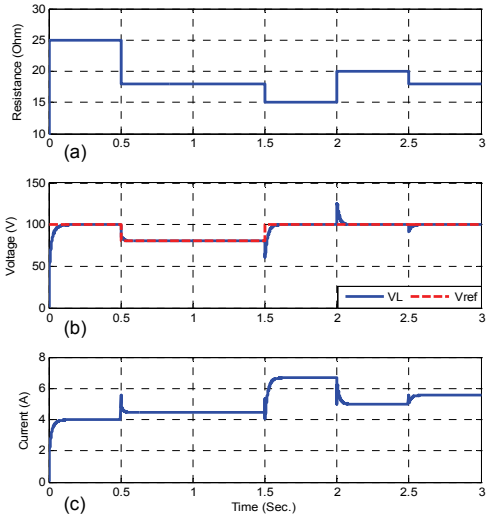


Fig. 6. (a). Load resistance, (b). DC bus, load voltage and DC bus voltage reference, (c). Load current

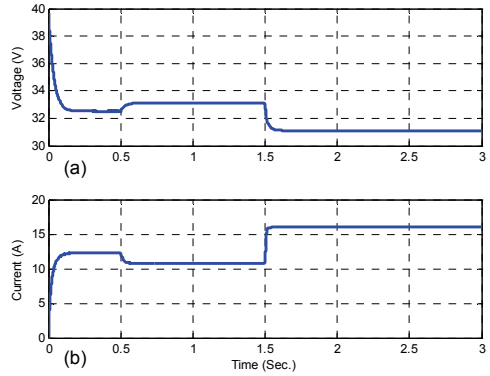


Fig. 7. Fuel cell voltage (a) and Current (b).

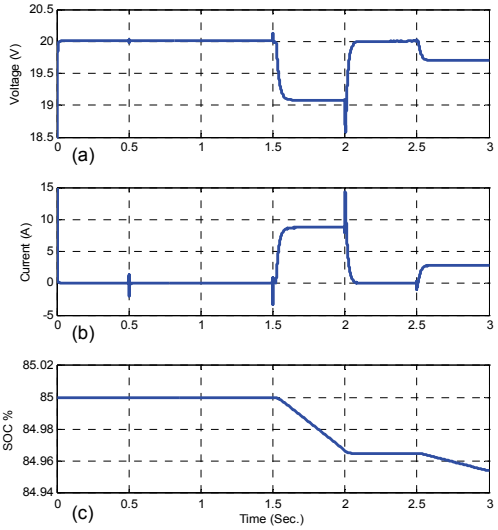


Fig. 8. (a). Battery voltage, (b). Battery current, (c). SOC of battery

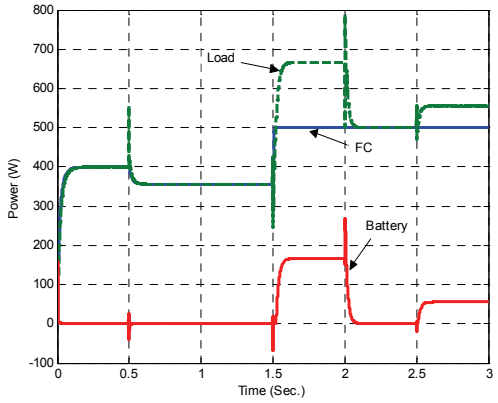


Fig. 9. Load, FC and battery power

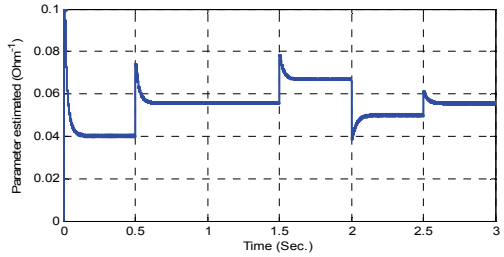


Fig. 10. Estimated value of $1/R_t$

In this study, it can be seen that the adaptive passivity-based controllers usage is reasonable for faster damping on FC/Battery system outputs due to the different disturbances, i.e. load resistance and DC bus voltage reference, see Fig. 9.

Similar results with aforementioned cases have been presented in [18] for adaptive passivity-based control of boost DC/DC converter. Also the results of quasi-resonant converter control via adaptive passivity-based control have been documented in [40] which demonstrate to verity of this study results.

## VII. Conclusion

In this paper, the Lagrangian modeling of a hybrid DC power source composed of a PEM fuel cell as main source, Li-ion battery storage as transient source and interfacing DC/DC converters have been presented. Subsequently, according to energy shaping and damping injection method, adaptive passivity-based controllers have been designed to control the interfacing DC/DC converters. Control of power flow between components has been done in the power management unit.

The proposed model has been validated by simulation results. Two cases have been studied, constant DC bus voltage reference and SOC%=70%, in this case, the battery storage, based on the load power situation, has cooperation to supply power to the load and absorb power from the fuel cell. In the second case, the DC bus voltage reference changes and SOC%=85%, therefore, the battery storage only supplies power to load.

The outputs of hybrid system in the both cases have low overshoot, short settling time and zero steady-state error. The aforementioned results demonstrate to the sufficiency of the proposed controllers.

## REFERENCES

[1]. Wang C, Nehrir MH, Shaw SR. Dynamic models and model validation for PEM fuel cells using electrical circuits. *IEEE Trans Energy Convers.,* 20 (2005), No. 2, 442-51.

[2]. Jiang Z, Dougal RA. A hybrid fuel cell power supply with rapid dynamic response and high peak-power capacity. *IEEE Applied Power Electronics Conference and Exposition*, (2006), 1250-1255.

[3]. Andujar JM, Segura M. Vasallo J. A suitable model plant for control of the set fuel cell DC/DC converter. *Renew. Energy*, 33 (2008), No. 4, 813-826.

[4]. Sharifi Asl SM, Rowshanzamir S, Eikani MH. Modelling and simulation of the steady-state and dynamic behavior of a PEM fuel cell. *Energy,* 35 (2010), No. 4, 1633–1646.

[5]. Khan MJ, Iqbal MT. Dynamic modeling and simulation of a small wind–fuel cell hybrid energy system. *Renew. Energy*, 30 (2005), No. 3, 421–439.

[6]. Amirabadi M, Farhangi SH. Fuzzy control of hybrid fuel cell/battery power source in electric vehicle. *IEEE Conference on Industrial Electronics and Applications,* (2006), 1-5.

[7]. Wang C, Nehrir MH, Gao H. Control of PEM fuel cell distributed generation systems. *IEEE Trans on Energy Convers.,* 21 (2006), No. 2, 586-595.

[8]. Uzunoglu M, Alam MS. Dynamic modeling, design and simulation of a PEM fuel cell/ultra-capacitor hybrid system for vehicular applications. *Energy Convers. Manage.,* 48 (2007), No. 5, 1544–1553.

[9]. Skvarenina TL. The Power Electronics Handbook; CRC Press, 2002

[10]. Jiang Z, Dougal RA. A compact digitally controlled fuel cell/battery hybrid power source. *IEEE Trans Ind. Elec.,* 53 (2006), No. 4, 1094-1104.

[11]. Li CH, Zhu XJ, Cao GY, Sui S, Hu MR. Dynamic modeling and sizing optimization of stand-alone photovoltaic power systems using hybrid energy storage technology. *Renew. Energy*, 34 (2009), No. 3, 815-826.

[12]. Gencoglu MT, Ural Z. Design of a PEM fuel cell system for residential application. *J. Hydrogen Energy,* 34 (2009), No. 12, 5242-5248.

[13]. Khan MJ, Iqbal MT. Dynamic modeling and simulation of a fuel cell generator. *Fuel Cells*, 5 (2004), No.1, 97-104.

[14]. El-Sharkh MY, Rahman A, Alam MS, Sakla AA, Byrne PC, Thomas T. Analysis of active and reactive power control of a stand-alone PEM fuel cell power plant. *IEEE Trans. Power Systems,* 19 (2004), No.4, 2022-2028.

[15]. Li YH, Choi SS, Rajakaruna S. An analysis of the control and operation of a solid oxide fuel-cell power plant in an isolated system. *IEEE Trans. Energy Convers.,* 20 (2005), No. 2, 381-387.

[16]. Onar OC, Uzunoglu M, Alam MS. Dynamic modeling, design and simulation of a wind/fuel cell/ultra-capacitor-based hybrid power generation system. *J. Power Sources,* 161 (2006), No. 2, 707-722.

[17]. Batlle C, Dòria-Cerezo A, Fossas E. Bidirectional power flow control of a power converter using passive hamiltonian techniques. *Int. J. Circ. Theor. Appl.*, 36 (2008), 769–788.

[18]. Kim DE, Lee DC, Feedback Linearization Control of Three-Phase AC/DC PWM Converters with LCL Input Filters, *The 7th International Conference on Power Electronics*, (2007), 766-771.

[19]. Mazumder SK, Nayfeh AH, Borojevic D. Robust control of parallel DC–DC buck converters by combining integral-variable-structure and multiple-sliding-surface control schemes. *IEEE Trans. Power Elec.,* 17 (2002), No. 3, 428-437.

[20]. Kim DE, Lee DC. Feedback linearization control of three-phase AC/DC PWM converters with LCL input filters. *7th International conference on power electronics,* (2007), 766-771.

[21]. Vmquez' N, Hernandez' C, Alvarez J, Arau J. Sliding mode control for DC/DC converters: A new sliding surface. *IEEE International Symposium on Industrial Electronics,* 1 (2003), 422-426.

[22]. Leyva R, Cid-Pastor A, Alonso C, Queinnec I, Tarbouriech S, Martinez-Salamero L. Passivity-based integral control of a boost converter for large-signal stability. *IEE Proc-Control Theory Appl.* 153 (2006), No. 2, 139-146.

[23]. Tofighi A, Kalantar M. Applying passivity-based control for the DC/DC converter of PEM fuel cell. *IEEE 1st Power Electronic & Drive Systems & Technologies Conference, (2010),* 439– 444.

[24]. Ortega R, Van Der Schaft A, Maschke B, Escobar G. Interconnection and damping assignment passivity-based control of port-controlled hamiltonian systems. *Automatica,* 38 (2002), No. 4, 585–596.

[25]. Scherpen JMA, Jeltsema D, Klaassens JB. Lagrangian modeling of switching electrical networks. *Systems & Control Letters,* 48 (2003), No. 5, 365–374.
[26]. A. Dòria-Cerezo, Modeling, Simulation and control of a Doubly-Fed Induction Machine Controlled by a Back-to-Back Converter, *PhD. Destination*, 2006, Technical University of Catalonia.
[27]. Kwasinski A, Krein PT. Passivity-based control of buck converters with constant-power loads. *IEEE Power Electronics Specialists Conference,* (2007), 259-265.
[28]. Wang P, Wang J, Xu Z. Passivity-based control of three phase voltage source PWM rectifiers based on PCHD model. IEEE *International Conference on Electrical Machines and Systems,* (2008), 1126-1130.
[29]. Lee TS. Lagrangian modeling and passivity-based control of three-phase AC/DC voltage-source converters. *IEEE Trans. Ind. Elec.,* 51 (2004), No. 4, 892-902.
[30]. Komurcugil H. Steady-state analysis and passivity-based control of single-phase PWM current-source inverters. *IEEE Trans. Ind. Elec.,* 57 (2010), No. 3, 1026-1030.
[31]. Ayad MY, Becherif M, Henni A, Aboubou A, Wack M, Laghrouche S. Passivity-based control applied to DC hybrid power source using fuel cell and supercapacitors. *Energy Convers. Manage.,* 51 (2010), No. 7, 1468–1475.
[32]. Sira-Ramirez H, Rios-Bolivar M, Zinober ASI. Adaptive dynamical input-output linearization of DC to DC Power converters: a backstepping approach. *Int. J. Robust and Nonlinear Control*, 7 (1997), 279-296.
[33]. Sira-Ramirez H, Ortega R, Garci-Esteban M. Adaptive passivity-based control of average DC-to-DC power converters models. Int. J. Adapt. Control Signal Process 1998; 12: 63-80.
[34]. Jeong KS, Lee WY, Kim CS. Energy management strategies of a fuel cell/battery hybrid system using fuzzy logics. *J. Power Sources,* 145 (2005), No. 2, 319–326.
[35]. Khateeb SA, Farid MM, Selman JR, Al-Hallaj S. Mechanical–electrochemical modeling of Li-ion battery designed for an electric scooter. *J. Power Sources,* 158 (2006), No. 1, 673–678.
[36]. Durr M, Cruden A, Gair S, McDonald JR. Dynamic model of a lead acid battery for use in a domestic fuel cell system. *J. Power Sources,* 161 (2006), No. 6, 1400–1411.
[37]. Chen M, Rinco'n-Mora GA. Accurate electrical battery model capable of predicting runtime and I–V performance. *IEEE Trans. Energy Convers.,* 21 (2006), No. 2, 504-511.
[38]. Escobar G, Ortega R, Sira-Ramirez H, Vilain JP, Zein I. An experimental comparison of several nonlinear controllers for power converters. *IEEE Control Systems Magazine,* 19 (1999), No. 1, 66-82.
[39]. Specifications of Polymer Lithium Ion Battery, Model: PL-383562.
[40]. Ho HF, Cheng KWE. Adaptive passivity-based control of extended-period quasi-resonant converters, IEEE International Conference on Power Electronics Systems and Applications, (2006), 260-265.

***Authors**: A. Tofighi, Department of Electrical Engineering, Iran University of Science and Technology, Tehran, Iran. E-mail: tofighi@iust.ac.ir, Tel.: +98 2177240540-50x2662; fax: +98 2177240354.*
*Prof. M. Kalantar, Department of Electrical Engineering, Iran University of Science and Technology, Tehran, Iran. E-mail: kalantar@iust.ac.ir, Tel.: +98 2177240540-50x5665; fax: +98 2177240354.*